ZnO/ZnO Core–Shell Nanowire Array Electrodes: Blocking of Recombination and Impressive Enhancement of Photovoltage in Dye-Sensitized Solar Cells

ARTICLE *in* THE JOURNAL OF PHYSICAL CHEMISTRY C · JUNE 2013

Impact Factor: 4.77 · DOI: 10.1021/jp402888y

7 AUTHORS, INCLUDING:

E. Guillén
Abengoa
29 PUBLICATIONS **710** CITATIONS
SEE PROFILE

Jesús Idígoras
Universidad Pablo de Olavide
23 PUBLICATIONS **183** CITATIONS
SEE PROFILE

Juan A Anta
Universidad Pablo de Olavide
109 PUBLICATIONS **1,800** CITATIONS
SEE PROFILE

Ramon Tena-Zaera
IK4-CIDETEC
73 PUBLICATIONS **2,420** CITATIONS
SEE PROFILE

THE JOURNAL OF PHYSICAL CHEMISTRY C

Article

pubs.acs.org/JPCC

ZnO/ZnO Core–Shell Nanowire Array Electrodes: Blocking of Recombination and Impressive Enhancement of Photovoltage in Dye-Sensitized Solar Cells

Elena Guillén,*[,†,∥] Eneko Azaceta,[‡] Alberto Vega-Poot,[†] Jesús Idígoras,[†] Jon Echeberría,[§] Juan A. Anta,[†] and Ramón Tena-Zaera*[,‡]

[†]Department of Physical, Chemical and Natural Systems, Universidad Pablo de Olavide, Sevilla 41013, Spain

[‡]Energy Division, IK4-CIDETEC, Parque Tecnológico de San Sebastián, Paseo Miramón 196, Donostia-San Sebastián 20009, Spain

[§]CEIT and TECNUN, University of Navarra, San Sebastián 20018, Spain

Supporting Information

ABSTRACT: A multistep wet-chemistry route was developed, by combining electrodeposition, colloidal synthesis and spin coating, to obtain arrays of ZnO nanowires (NWs) coated by a ZnO nanocrystalline layer (i.e., ZnO/ZnO core–shell NWs). They were integrated as anodes in dye-sensitized solar cells. With the use of an iodide-based electrolyte, photovoltages as impressive as 870 mV were obtained with an enhancement of more than 250 mV with respect to devices based on bare NWs. A comprehensive device characterization study by means of impedance spectroscopy (EIS) and intensity-modulated photovoltage spectroscopy (IMVS) reveals a significant blockage of recombination upon NW shell deposition. To study the generality of this multistep method, electrodes of core–shell nanostructures based on commercial ZnO nanoparticles were also prepared. A decrease of recombination rate is also detected, although it is much more moderate than the observed for nanowire-based electrodes. The present ZnO synthetic approach allows obtaining nanowire-based dye-sensitized solar cells which exhibit longer electron lifetimes than nanocrystalline analogues. This finding implies a significant improvement of photovoltage with respect to the state of the art ZnO-based dye-sensitized solar cells.

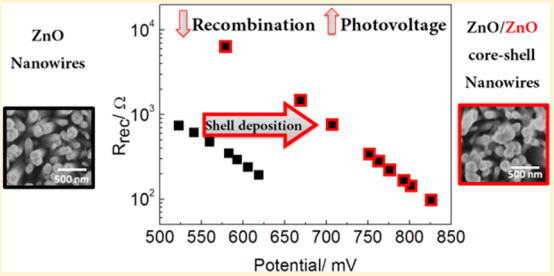

1. INTRODUCTION

In recent years, ZnO nanowire (NW) arrays have attracted increasingly more attention in the field of energy conversion due to their great potential to be used as emerging building blocks in several devices such as solar cells[1−3] or piezoelectric nanogenerators[4] and also for storage[5,6] and saving.[7] Their unique combination of physical properties and availability to be obtained by wet-chemistry deposition, i.e., low-cost and large-scale compatible methods, has enormously encouraged the research on this material. Until now, several proofs of concept of innovative devices[1,7−11] have been shown, opening fascinating new research fields.[12] However, further improvements related to tailoring of ZnO NW array properties and device integration are still necessary to make multifunctional building blocks technologically competitive.

In particular, the use of ZnO NW arrays as electrodes for dye-sensitized solar cells (DSCs) is a current and very active research topic. However, DSCs based on ZnO NWs and other one-dimensional (1D) nanostructures have not reached as high conversion efficiencies as expected. A recurrent explanation for the low performance of ZnO NW arrays-based DSC is the low surface area available for dye adsorption in 1D nanostructures. However, a recent report[13] showed that bare NWs can reach absorptances comparable with standard nanoparticle-based electrodes if a high extinction coefficient dye is used. Furthermore, the surface area can be significantly enhanced by using nanowire/nanoparticle composites[14,15] and NW-based hierarchical electrodes.[16−21] By this route DSCs which exhibit photocurrents comparable to those of ZnO nanoparticle-based electrodes have been fabricated.[14,17,22−24] Nevertheless, the photovoltages achieved for ZnO NW-based DSC (including their NW/NP composites and hierarchical derivates) are systematically lower than the ones obtained for cells based on ZnO NP-based electrodes.[25] Indeed, a high recombination rate rather than a low surface area has been recently pointed out as the main limitation for DSC based on the aforementioned ZnO NWs sensitized with high extinction coefficient dyes.[13] A high concentration of surface states on the NWs, which seems to be a common feature in those obtained by wet-chemistry synthetic methods, was considered as the main reason for the high recombination losses.

In principle, coating NWs by a thin film (i.e., NW shell) may be an efficient way to passivate NW surface defects. Significant improvement of photovoltage has been observed for DSCs based on ZnO/TiO_2 core–shell NW arrays,[1,26,27] although much more moderate improvements have been found with

Received: March 24, 2013
Revised: May 29, 2013
Published: June 5, 2013

shells based on different oxides (e.g., Al_2O_3, MgO and ZrO_2).[28−30] Regarding the photocurrent a strong dependence on the thickness and crystalline quality of the TiO_2 shell has been pointed out by different groups.[26,28] Due to this fact the use of deposition techniques such as Atomic Layer Deposition (ALD) has been suggested. In addition, a very recent report[31] proposes that in spite of their longer electron lifetimes with respect to bare nanorods, the efficiency of core−shell devices may be limited by the presence of an energy barrier which blocks electron transfer from wet-chemically deposited TiO_2 nanoparticles to ZnO nanorods. This idea is supported by accurate studies[32,33] on core−shell nanoparticle-based DSCs which demonstrate that, additionally to surface defects passivation, the shell may induce different phenomena such as the formation of an energy barrier, but also a surface dipole layer and the consequent shift in the conduction band of the core. In line with this, a defect passivation strategy based on a cheap and simple wet-chemistry approach (in contrast to potentially expensive and energy-consuming techniques, such as ALD), and without the need of including a different metal oxide may be highly attractive from a technical and a fundamental point of view. This paper reports on a facile multistep wet-chemistry route to obtain arrays of ZnO NWs coated by a ZnO nanocrystalline layer (i.e., ZnO/ZnO core−shell NWs) and their use as electrodes in dye-sensitized solar cells. Photovoltages as impressive as 870 mV using an iodide-based electrolyte are obtained with an enhancement of more than 250 mV with respect to devices based on bare NWs. To the best of our knowledge, this represents the record photovoltage obtained for a ZnO-based DSC, including devices with a cobalt-based electrolyte,[34] despite the well-known better match between the cobalt complex redox potential and the oxidation potential of the dyes usually used in DSC in comparison to the iodide/triiodide redox couple. An extensive small-signal electrochemical study points to a significant blockage of recombination upon shell deposition. To study the applicability of the method, electrodes of core−shell nanostructures based on commercial ZnO nanoparticles were also prepared. A decrease of recombination was also detected for these electrodes, although much more moderate than for NW based electrodes.

2. EXPERIMENTAL SECTION

The NW arrays were electrodeposited as explained elsewhere.[13] The cathode was a commercial conducting glass/SnO_2:F (TEC15, Hartford Glass Co) substrate, which was previously covered by a thin continuous ZnO sprayed layer. Two different NW lengths (2 and 5 μm) were prepared by varying the charge density. The as-grown NWs samples were washed with acetone and isopropanol and then annealed to 450 °C for 30 min. The NW shell was deposited from a ZnO colloidal suspension, prepared according to Pacholski method as explained elsewhere,[35] which consisted of spin coating at 2000 rpm for 30 s on the NW array samples. Each deposition process was followed by annealing the sample at 100 °C in air for 5 min. The spin coating and annealing is referred as a *cycle* and a series of cycles were studied (i.e., 0, 10, 25, 30, and 50).

Commercial ZnO nanoparticles were used to fabricate the nanoparticle-based electrodes and details of the film preparation can be found elsewhere.[36] Similar procedure to that applied on NW arrays was followed to prepare core−shell nanoparticle based electrodes.

Sensitization of the ZnO anodes was performed by immersing the electrodes in a solution 0.5 mM of indoline dyes known as D149 or D358 (Mitsubishi Paper Mills Limited) and 0.7 mM of chenodeoxycholic acid for 60 min in *tert*-butyl alcohol/acetonitrile. The electrolyte was composed of 0.05 mM I_2 and 0.5 M TBAI in acetonitrile/ethylencarbonate (1:4). Also an electrolyte with the inverse proportion of both solvents (acetonitrile/ethylencarbonate (4:1) was employed in some cases, which are indicated in the text. The counter electrode was prepared by spreading 15 μL of Platisol (Solaronix) on the conductive side of TEC8 electrodes and subsequent annealing at 400 °C for 5 min. The electrodes and counter electrodes were sealed together with a Surlyn thermoplastic film frame (25 μm, Solaronix). The cell area was 0.49 cm^2 in all the samples studied.

The morphology of the ZnO electrodes was analyzed using a Field Emission Scanning Electron Microscope (ULTRA plus ZEISS FESEM). A JEOL JEM 2100 Transmission Electron Microscope, with an accelerating potential of 200 kV, was used for further morphology and structural analyses. Thin lamellas from core−shell ZnO nanowire arrays were prepared by Focused Ion Beam (FIB) in a QUANTA 3D FEG system from FEI. The nanowire arrays were previously embedded in a CuSCN matrix[37] in order to facilitate the preparation of the cross section lamellas. The surface of the samples was protected from the Ga-ion beam by the deposition of a platinum layer of 2 μm thickness. The thinning process up to a thickness of 20−30 nm was performed by a high energy ion beam (30 KV), followed by a cleaning process using low-energy ions (1−2 KV). The lamellas were welded on a lift-out copper grid with an Omniprobe Autoprobe 100.7 micromanipulator. The current−voltage characteristic of the cells was measured using a solar simulator (ABET), and the intensity was adjusted to provide 1 sun (100 mW cm^{-2}) using a calibrated silicon solar cell. Electrochemical Impedance Spectroscopy (EIS) measurements under illumination were carried out by means of an Autolab/PGSTAT302N station (Echochemie) coupled with a FRA2 frequency generator module. A high intensity green light-emitting diode (LED LUXEON, collimated, 540 nm) was employed to illuminate the DSCs. EIS measurements were performed using a 10 mV perturbation in the 10^{-2}−10^6 Hz range. Zview equivalent circuit modeling software was used to fit the data. Intensity Modulated Photovoltage Spectroscopy (IMVS) measurements were carried out by coupling the PGSTAT302N/FRA2 module to the light emitting diode. IMVS measurements were performed at open circuit in the 10^4−10^{-1} Hz range with a light perturbation corresponding to 10% of the DC background illumination intensity. In all cases, the samples were illuminated from the dye-coated ZnO electrode side.

3. RESULTS AND DISCUSSION

3.1. Characterization of ZnO-ZnO Core−Shell NWs.

Figure 1 shows the SEM micrographs of ZnO NW arrays before (a) and after colloidal nanoparticle deposition of different number of spin coating cycles (b, 30 cycles; c, 50 cycles). In general, a quite homogeneous coating for all the NWs forming the array is observed. A slight coarsening between neighboring NWs is only detected for samples with 50 cycles of deposition. Higher magnification micrographs (Figure 1d−g) suggest that the nanoparticle coating is homogeneous, in the form of a shell, along each NW. This is supported by the cross section SEM micrographs (Figure S1).

dx.doi.org/10.1021/jp402888y | J. Phys. Chem. C 2013, 117, 13365−13373

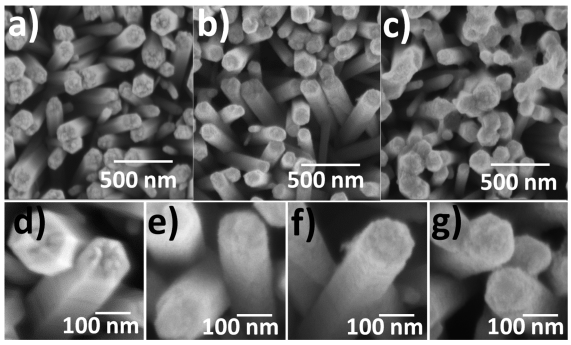

Figure 1. SEM micrographs of bare ZnO NWs (a and d) and ZnO-ZnO core–shell NWs with 30 (b and f), 50 (c and g), and 10 (e) spin coating cycles.

As a further evidence, Figure 2 shows bright field and high resolution Transmission Electron Microscopy (TEM) micrographs of a NW after 10 (a and b) and 50 (c and d) spin coating cycles. By comparing with TEM micrographs of bare NWs (Figure S2), an increase of the surface roughness was detected after 10 cycles deposition process (Figure 2a). However, the HRTEM micrographs (Figure 2b) did not show any significant variation of the lattice fringe pattern at the nanowire edge. Indeed, the higher contrast feature detected along the NW walls suggests the presence of a very thin (i.e., < 1 nm) epitaxial-like shell. Taking into account the small size of the colloidal nanoparticles (i.e., ~ 3 nm)[38] and their affinity to the ZnO NW surface, an expitaxial-like shell growth could occur during the soft thermal annealing included in each spin coating cycle. An ~10 nm thick shell, which is mainly constituted of ~3–5 nm diameter nanoparticles, was clearly detected in HRTEM micrographs of 50 cycles coated NWs (Figure 2c).

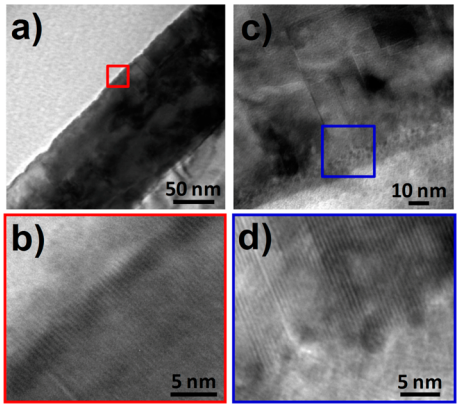

Figure 2. Bright field and high resolution TEM micrographs of ZnO nanowires coated with 10 (a and b) and 50 (c and d) spin coating cycles.

Thus, homogeneous arrays of ZnO/ZnO core–shell NWs were obtained by combining two wet-chemistry routes. It is worthy of mention that the stability of the NW shell to the dye-sensitization process was analyzed by desorbing dye molecules and comparing the resulting ZnO morphology with respect to the original one. No significant differences were detected by FE-SEM (Figure S3), which suggests that dye-sensitization did not significantly damage the shell.

3.2. Photovoltaic Performance. The effect of the NW shell on the photovoltaic behavior of solar cells was analyzed. DSC based on arrays of 2.5 μm length NWs coated by a different number of spin coating cycles (i.e., 0 (bare NWs), 25 or 50) were prepared. The dye employed in this study was D149, and a similar analysis was carried out for electrodes sensitized with D358, but only for bare and core–shell NWs with the highest number of cycles (i.e., 50). The photovoltaic performances were evaluated by measuring the current–voltage characteristic under 1 sun light illumination (AM 1.5). The dependence of the different photovoltaic parameters on the number of spin coating cycles was analyzed. At least three cells with each type of electrodes were fabricated. Mean values from this analysis and their standard deviations are represented in Figure 3.[39]

Although a slight increase of the photocurrent (J_{sc}) was generally detected for core–shell NW-based solar cells, the variation is in the order of the data dispersion (Figure S4). This fact makes it difficult to conclude a clear trend as a function of the shell cycle number as occurred in the estimations of the loaded dye (Table S1), which suggests no significant enhancement of surface area as a function of the number of deposition cycles. In contrast, a clear improvement of *FF* (Figure 3a) and V_{oc} (Figure 3b) as a function of the shell cycle number was detected. V_{oc} values over 700 and 870 mV (for D149 and D358, respectively) were obtained for 50 cycles core–shell NWs. As pointed above, the latter is to our knowledge, the highest photovoltage obtained for a ZnO-based DSC.

Although both dyes are quite similar (see Figure S5) and exhibit similar extinction coefficients (D149, 68 700 mol^{-1} cm^{-1} at 526 nm[40] and D358, 67 000 mol^{-1} cm^{-1} at 532

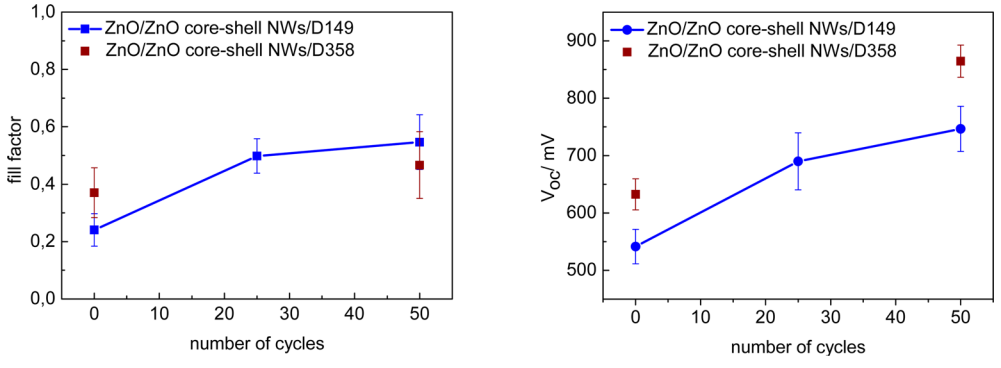

Figure 3. Trend of the fill factor and the photovoltage as a function of the number of spin coating cycles for 2.5 μm length nanowire-based electrodes sensitized with D149 or D358.

dx.doi.org/10.1021/jp402888y | J. Phys. Chem. C 2013, 117, 13365–13373

nm),[41] D358 attaches onto ZnO surface via two carboxilyc groups, whereas D149 exhibits only one site of adsorption. This fact, together with the longer aliphatic chains of D358, could lead to a better coverage of the oxide surface and a steric exclusion of electron acceptors on the electrolyte side.[42] Both effects would lead to lower recombination rates for D358 dye and could explain the larger photovoltage.

Thus, ZnO/ZnO core−shell NWs here reported make it possible to reach an impressive enhancement of photovoltage (i.e., > 150 mV) with respect to the state of the art of ZnO-based DSCs with an iodide-based electrolyte, including those based on nanostructures obtained after multistep deposition processes such as nanowire/nanoparticle composites[14,15] and NW-based hierarchical architectures,[19,20,43] and also higher than the photovoltages reported very recently by Hagfeldt et al. for ZnO DSCs with a cobalt-based electrolyte.[34] Indeed, V_{oc} values here reported are higher than those attained previously for ZnO/TiO_2 core−shell NWs.[26,28] It is worth to remark the low cost and technical simplicity of the present approach with respect to ALD, a technique which is generally used for the deposition of TiO_2 shells. The better tolerance of photocurrent to shell thickness, due to the likely absence of energy barriers, may also be a significant advantage of the present ZnO/ZnO core−shell nanostructures.

Figure 4 shows the IV characteristics for DSCs based on ZnO/ZnO core−shell (50 cycles) NWs of 5 μm length

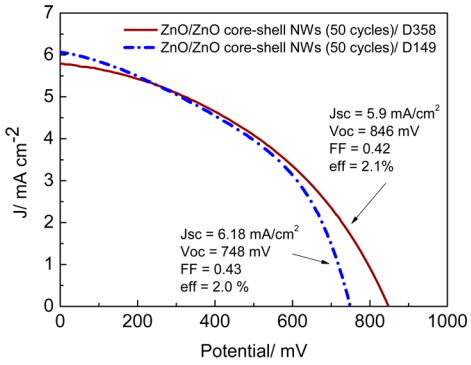

Figure 4. IV characteristics for DSCs fabricated using ZnO-ZnO core−shell NWs 5 μm length electrodes with 50 deposition cycles and sensitized with one of the two different indoline dyes used in this study. The electrolyte was composed of 0.05 mM I_2 and 0.5 M TBAI in acetonitrile/ethylencarbonate (4:1).

sensitized with D149 or D358 dyes. The photovoltaic parameters can also be found in the figure. An efficiency of 2.1% is obtained with 5 μm length NWs. However, the most remarkable result is observed, again, in the photovoltage, which is more than 800 mV with no additives present in the electrolyte such as 4-tert-butylpyridine (TBP) or ionic liquids which are known to have a positive effect on the open circuit potential. The similar photovoltage obtained for 2.5 and 5 μm length core−shell NWs, and the systematic increase of V_{oc} upon the number of cycles (Figure 3), not accompanied by larger dye loading (Table S1), are further indications that the main effect of the coating is surface modification and not the increase in the surface area (i.e., photovoltage enhancement due to higher photocurrent).

3.3. Recombination Losses in ZnO-ZnO Core−Shell Nanowire-Based Solar Cells. To cast some light into the reasons for the positive effect of the NW shell, solar cells based on NWs with different shell deposition cycles were analyzed by electrochemical impedance spectroscopy. Measurements were carried out at open circuit over a wide range of light intensities. In experiments performed in the open circuit mode, the applied voltage corresponds to the V_{oc} observed at the intensity of the incident light. Hence, at this voltage, there is no net current flow and no correction of the IR drop needs to be considered. Figure 5 shows the Nyquist diagrams obtained from EIS characterization of DSCs based on bare and 50 cycles core−shell NWs 5 μm in length sensitized with D358 dye.

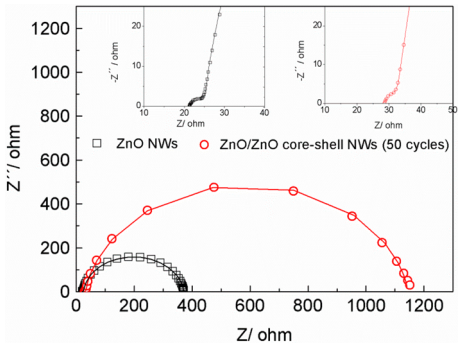

Figure 5. Nyquist plots obtained from impedance measurements of cells based on bare NWs and ZnO/ZnO core−shell NWs (50 cycles). Measurements were carried out under illumination, and both spectra correspond to a similar photovoltage induced by illumination (~580 mV). A magnification of the high frequency region is included in the insets to show the accuracy of the fitting.

Both photoanodes exhibit similar light harvesting (Figure S6) and both impedance spectra correspond to a similar photovoltage induced by illumination. In the Nyquist plot, the characteristic midfrequency semicircle (right side of the spectrum), attributed to charge transfer at the oxide−electrolyte interface, and an additional arc at high frequencies (left side of the spectrum, see inset in Figure 5) accounting for the counter electrode can be clearly observed. The spectra were fitted to the equivalent circuit shown in Figure S7a. The different elements have the following physical meaning: R_s is the series resistance of the cell, R_{rec} and C_μ are the recombination charge transfer resistance and the chemical capacitance at the oxide/electrolyte interface, and R_{pt} and C_{pt} are the charge transfer resistance and the double layer capacitance at the electrolyte/counter electrode interface.

In Figure 6, R_{rec} is plotted as a function of the photovoltage for the studied samples. In both cases, this parameter follows an approximate exponential behavior, according to $R_{rec} = R_0 \exp(-\beta q/VkT)$, with β being the transfer parameter. From the experimental slopes, a transfer parameter ~0.4 is found for both devices. In agreement with the spectra shown in Figure 5, the core−shell NW-based cell exhibits much more resistance to recombination at the same voltage generated by illumination. A similar trend in R_{rec} was found for 2.5 μm length NWs with different numbers of shell cycles and sensitized with one of the tested dyes (D149 or D358, Figure S8). The behavior observed in Figure 6 hence summarizes the effect of the NW shell. In all the cases, no matter the NW length or the dye employed, there is an increase on the resistance to recombination upon shell deposition.

An increase of the recombination resistance was also previously suggested for DSC based on ZnO/TiO_2 core−shell NWs,[26,28] although there were no detailed reports on

dx.doi.org/10.1021/jp402888y | J. Phys. Chem. C 2013, 117, 13365−13373

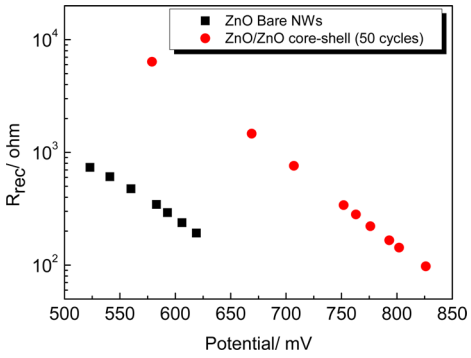

Figure 6. R_{rec} as a function of photovoltage for bare NWs and ZnO/ZnO core−shell NWs (50 cycles) sensitized with D358 dye.

impedance spectroscopy characterization. However, accurate studies on DSC built from anodes based on core−shell NPs constituted of two different oxides pointed out that recombination blocking takes place due to the formation of a dipole layer at the core−shell interface.[33] Apart from differences in the conduction band energy, the formation of the surface dipole layer could be due to differences between the core and shell materials with respect to their acidity or electron affinity.[33] However, the present approach provides a new pathway to decrease recombination without need of combining different metal oxides. A NW shell is deposited in order to decrease the density of available surface states in bare NWs. Present results contribute significant progress and novelty with respect to other approaches based on combination of different ZnO deposition techniques. With respect to NWs-NPs composite electrodes, some authors have reported the reduction of recombination in this hierarchical structures.[23] However, the V_{oc} increment was much lower than the reported here, and the fill factor was hardly affected. In fact, most of DSCs based on NW-NP ZnO composite electrodes led very often to a great diminishing of the resistance to recombination with respect to bare NWs.[44,45] The decrease in charge-transfer resistance is usually attributed to an increase in the interface area available for recombination or to the introduction of additional interfaces and surface traps which can act as recombination centers. In those cases, when a better photovoltage is obtained, it is ascribed to enhanced light harvesting as a consequence of the higher surface area.[46]

Electron lifetimes have been obtained from impedance measurements according to $\tau_n = R_{rec}C_\mu$. The obtained lifetimes are plotted versus the photovoltage in Figure 7. With respect to

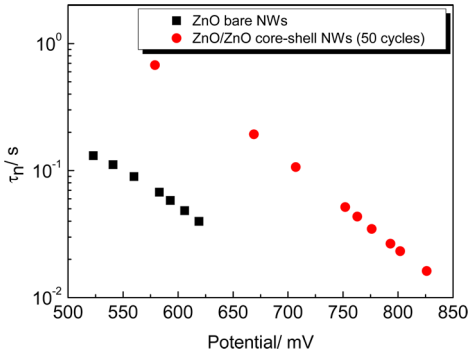

Figure 7. τ_n as a function of the photovoltage for bare NWs and ZnO/ZnO core−shell NWs (50 cycles) sensitized with D358 dye.

capacitance, although it shows the typical behavior of a chemical capacitance (Figure S11b),[47] reflecting accumulation of electrons in an exponential distribution of localized states, the absolute value of C_μ is found to depend strongly on the particular sample studied. Considering that the capacitance is also a function of the number of surface states available for charge accumulation, this observation is in fact consistent with the aforementioned dispersion of data detected for the photocurrents and dye loadings. Hence, it was not possible to establish the occurrence of band shifts,[36,48] although they are not expected to be decisive to explain the clear correlation between open-circuit voltage and recombination resistance with respect to the number of deposition cycles.

Additionally, lifetimes were also obtained from intensity-modulated photovoltage spectroscopy (IMVS). Both methods (EIS and IMVS) yield practically the same lifetimes values (Figure S9), which is an indication of the accuracy of our EIS fitting and the suitability of the equivalent circuit employed.

The longer lifetimes would explain the much higher photovoltages and also the improvement in the fill factors upon shell deposition. However, low FF values in DSC are not necessarily due to a high recombination rate.[49] FF may be specially limited by the slower injection potentially induced by the relatively high ZnO dielectric constant with respect to the most often used TiO_2-based DSC anodes,[36] and potentially affected by the particular radial profile of free carrier concentration in ZnO NWs.[37]

3.4. ZnO-ZnO Core−Shell Nanoparticles Based Electrodes. The effect of shell deposition on NW array-based anodes has been clearly elucidated in the previous section. To gain further insight into the generality of the present approach, a similar study was carried out for randomly oriented nanoparticle-based electrodes. Briefly, a ZnO nanoparticle colloidal suspension has been spin coated on the nanoparticle-based anodes. As an example, Figure 8 shows the SEM

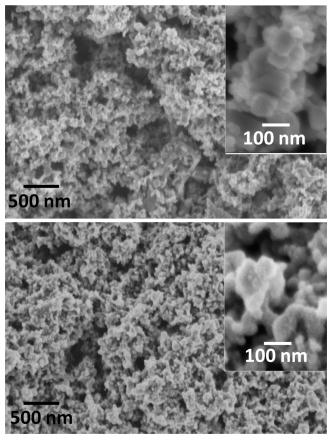

Figure 8. SEM micrographs of a nanoparticle-based electrode before (a) and after (b) 50 spin coating cycles.

micrograph of an anode before (a) and after 50 spin coating cycles (b). Significant roughness is detected after spin coating deposition, which suggests the formation of a nanocrystalline shell on the nanoparticles surface. For DSC fabrication, the best performing indoline dye, D358, was chosen as a sensitizer. Although no clear increment of the photocurrent is observed, significant enhancement in photovoltage was detected when

dx.doi.org/10.1021/jp402888y | J. Phys. Chem. C 2013, 117, 13365−13373

measuring current−voltage curves of DSC based on spin coating anodes (Figure S10).

Figure 9 displays the photovoltage and fill factor as a function of the number of cycles. Once again, a clear positive effect on

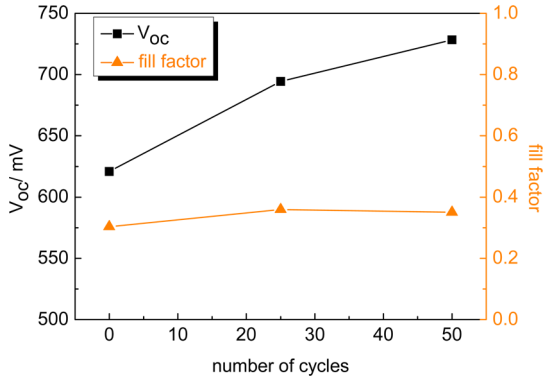

Figure 9. Trend of the photovoltage and the fill factor as a function of the number of spin coating cycles for nanoparticle-based electrodes sensitized with D358.

the photovoltage is obtained upon shell deposition. However, the improvement with respect to the bare nanoparticle electrode (~100 mV) is much more moderate than in the case of NWs (>250 mV) with the same sensitizer. The fill factor is hardly affected. An accurate study by impedance spectroscopy of this type of electrodes was also carried out, using the equivalent circuit shown in Figure S7b for spectra fitting. Although shell deposition increased the resistance to recombination with respect to anodes based on bare commercial nanoparticles (Figure S11), the increment is not as high as that observed for NWs. This could explain the much better photovoltages obtained with core−shell NW-based anodes using the same dye and electrolyte (Figure 3).

As explained below, a lower effect of the deposition of the shell on nanoparticle-based anodes was expected. On the one hand, it must not be forgotten that the nanostructures analyzed here as base electrodes (NPs and NWs) are fabricated by different methods. The chemical structure of the ZnO surface will depend to a great extent on the synthetic procedure. NWs were electrodeposited in aqueous media. In contrast, the commercial powders were synthesized in the gas phase.[50] As proved by photoluminescence,[51−53] gas phases synthetic approaches result in lower donor density (i.e., density of surface states). Therefore, the donor density (i.e., density of surface states) is expected to be lower in commercial NPs than in NWs. On the other hand, due to the mesoporous disorder structure of the nanoparticles electrode, a homogeneous shell is not formed on the surface of the nanoparticles placed deep in the anode (Figure S12), whereas the aligned nature of the nanowire arrays favors the penetration of the spin coating nanoparticles (Figure S1). Despite these facts, an improvement of the surface properties seem to be induced by the shell deposition even in gas phase synthesized ZnO nanoparticles.

Taking into account the R_{rec} and C_{μ} obtained by impedance spectroscopy (Figure S11), the electron lifetime was calculated. A significant enhancement of the electron lifetime was detected in DSC built from spin coated nanoparticle-based anodes (Figure 10). Thus, evidence of the generality of the present approach (i.e., ZnO nanocrystalline shell deposition) on anodes with different morphology and properties is given.

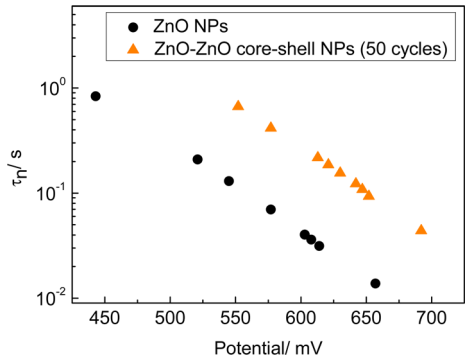

Figure 10. τ_n as a function of the photovoltage for a bare NP-based electrode and a ZnO/ZnO core−shell NPs (50 cycles) electrode sensitized with D358 dye.

Interestingly, the comparison of electron lifetime (Figure 11) for DSC based on different ZnO/ZnO core−shell nanostructures points out longer values (i.e., slower recombination dynamics) for core−shell NW architecture.

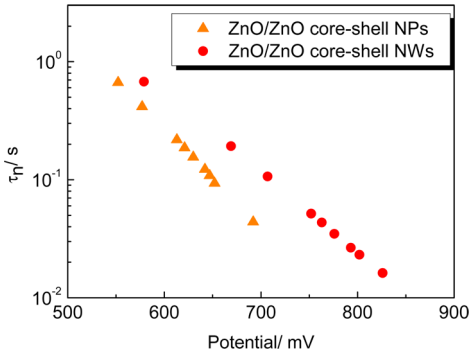

Figure 11. τ_n as a function of the photovoltage for ZnO/ZnO core−shell NPs (50 cycles) and ZnO/ZnO core−shell NWs (50 cycles) sensitized with D358 dye.

To the best of our knowledge, this is the first time that ZnO NW array-based anodes make it possible to reach longer electron times than those based on randomly oriented ZnO nanoparticles. This is a clear evidence of the major relevance of NW surface control on the DSC recombination dynamics. The slowdown of recombination dynamics by a simple spin coating method appears to be the pending piece of the puzzle for enhancing the electron diffusion length (i.e., $L_n = (D_n\tau_n)^{1/2}$, where D_n is the effective diffusion coefficient for the electron), by taking advantage of the faster electron transport already demonstrated in ZnO nanowires by several research groups.[54,55] It is worth to note that, in previous studies,[54,55] a relatively fast recombination dynamics in ZnO NW-based DSC impeded improvements in electron diffusion length and consequently in charge collection efficiency with respect to the nanoparticle-based analogue DSC. Although the charge collection efficiency is high (i.e., close to 100%) in the latter when high diffusion electrolytes are used, this may be a major limitation for the successful development of DSC using diffusion-limited hole transport materials (e.g., cobalt based electrolytes[56,57] and solid state hole conductors),[58] which are now attracting growing interest due to recent promising results.[59] The improved photovoltaic performance reported for P3HT/PCBM bulk heterojunction solar cells based on similarly surface modified ZnO NWs[60] seems to point toward the

dx.doi.org/10.1021/jp402888y | J. Phys. Chem. C 2013, 117, 13365−13373

feasibility of the present approach in excitonic solar cells in general.

4. CONCLUSION

Arrays of ZnO nanowires coated with a ZnO nanocrystalline layer (i.e., ZnO/ZnO core−shell NWs) were successfully obtained by a multistep wet-chemistry route based on a proper combination of electrodeposition, colloidal synthesis and spin coating techniques. The use of ZnO/ZnO core−shell NWs as advanced anodes in dye-sensitized solar cells was investigated. The NW shell deposition resulted in an enhancement of more than 250 mV in DSC photovoltage with respect to devices based on bare NWs, reaching values of 870 mV. The latter provides a significant improvement of photovoltage (i.e., > 150 mV) with respect to the state of the art of ZnO-based dye-sensitized solar cells based on iodide electrolyte in general (i.e., not only those based on NWs), and it is also higher than ZnO-based DSCs with cobalt electrolytes. An extensive DSC characterization study using impedance spectroscopy and intensity-modulated photovoltage spectroscopy showed a significant slowdown of the recombination dynamics in DSC based on core−shell NW arrays. To study the generality of the ZnO shell-based approach, electrodes of core−shell nanostructures based on commercial ZnO nanoparticles were also prepared and a decrease of recombination was also detected although much more moderate than for nanowire based electrodes. Altogether, a wet-chemistry approach (commonly regarded as a low-cost technique) was developed in order to modify the ZnO NW surface, providing a clear evidence of the major relevance of NW surface properties on the interface recombination dynamics and, therefore, on the DSC performance. Present results may have special impact on DSC based on hole transport materials with mass transport limitations (e.g., cobalt based electrolytes and solid state hole conductors). The slowdown of recombination dynamics by a simple spin coating method appears to be the pending piece of the puzzle for enhancing the performance of ZnO-based Dye-sensitized Solar Cells (DSCs).

■ ASSOCIATED CONTENT

Supporting Information

SEM micrographs of ZnO NWs, ZnO-ZnO core−shell NWs and nanoparticle based electrodes, high resolution TEM micrographs of ZnO-ZnO core−shell NWs and additional photovoltaic and impedance spectroscopy data. This material is available free of charge via the Internet at http://pubs.acs.org.

■ AUTHOR INFORMATION

Corresponding Author

*E-mail: (E.G.) meguirod@upo.es, (R.T.-Z.) rtena@cidetec.es.

Present Address

[‖]E. Guillén: Abengoa Research, Campus Palmas Altas, 41014, Sevilla, Spain, elena.guillen@research.abengoa.com.

Notes

The authors declare no competing financial interest.

■ ACKNOWLEDGMENTS

We thank the Ministerio de Educación and Ciencia of Spain for project HOPE CSD2007-00007 (Consolider-Ingenio 2010) and the Basque Regional Government through Etortek Program. R.T.-Z. acknowledges the support from the Program "Ramón and Cajal" of the MICINN.

■ REFERENCES

(1) Law, M.; Greene, L. E.; Johnson, J. C.; Saykally, R.; Yang, P. Nanowire Dye-sensitized Solar Cells. *Nat. Mater.* **2005**, *4*, 455−459.

(2) Gonzalez-Valls, I.; Lira-Cantu, M. Vertically-aligned Nanostructures of ZnO for Excitonic Solar Cells: A Review. *Energy Environ. Sci.* **2009**, *2*, 19−34.

(3) Lévy-Clément, C.; Tena-Zaera, R.; Ryan, M. A.; Katty, A.; Hodes, G. CdSe-Sensitized p-CuSCN/Nanowire n-ZnO Heterojunctions. *Adv. Mater.* **2005**, *17*, 1512−1515.

(4) Wang, Z. L.; Song, J. Piezoelectric Nanogenerators Based on Zinc Oxide Nanowire Arrays. *Science* **2006**, *312*, 242−246.

(5) Wang, H.; Pan, Q.; Cheng, Y.; Zhao, J.; Yin, G. Evaluation of ZnO Nanorod Arrays with Dandelion-like Morphology as Negative Electrodes for Lithium-Ion Batteries. *Electrochim. Acta* **2009**, *54*, 2851−2855.

(6) Kushima, A.; Liu, X. H.; Zhu, G.; Wang, Z. L.; Huang, J. Y.; Li, J. Leapfrog Cracking and Nanoamorphization of ZnO Nanowires during in Situ Electrochemical Lithiation. *Nano Lett.* **2011**, *11*, 4535−4541.

(7) Könenkamp, R.; Word, R. C.; Godinez, M. Ultraviolet Electroluminescence from ZnO/Polymer Heterojunction Light-Emitting Diodes. *Nano Lett.* **2005**, *5*, 2005−2008.

(8) Liao, L.; Lu, H. B.; Li, J. C.; He, H.; Wang, D. F.; Fu, D. J.; Liu, C.; Zhang, W. F. Size Dependence of Gas Sensitivity of ZnO Nanorods. *J. Phys. Chem. C* **2007**, *111*, 1900−1903.

(9) Wang, X. D.; Zhou, J.; Lao, C. S.; Song, J. H.; Xu, N. S.; Wang, Z. L. In Situ Field Emission of Density-Controlled ZnO Nanowire Arrays. *Adv. Mater.* **2007**, *19*, 1627−1631.

(10) Wang, X.; Song, J.; Liu, J.; Wang, Z. L. Direct-Current Nanogenerator Driven by Ultrasonic Waves. *Science* **2007**, *316*, 102−105.

(11) Badre, C.; Pauporté, T. Nanostructured ZnO-Based Surface with Reversible Electrochemically Adjustable Wettability. *Adv. Mater.* **2009**, *21*, 697−701.

(12) Wang, Z. L. *Nanogenerators for Self-Powered Devices and Systems*; Georgia Institute of Technology: Atlanta GA, 2011.

(13) Guillén, E.; Azaceta, E.; Peter, L. M.; Arnost, Z.; Tena-Zaera, R.; Anta, J. A. ZnO Solar Cells with an Indoline Sensitizer: a Comparison Between Nanoparticulate Films and Electrodeposited Nanowire Arrays. *Energy Environ. Sci.* **2011**, *4*, 3400−3407.

(14) Yodyingyong, S.; Zhang, Q.; Park, K.; Dandeneau, C. S.; Zhou, X.; Triampo, D.; Cao, G. ZnO Nanoparticles and Nanowire Array Hybrid Photoanodes for Dye-sensitized Solar Cells. *Appl. Phys. Lett.* **2010**, *96*, 073115.

(15) Zhang, Q.; Cao, G. Nanostructured Photoelectrodes for Dye-Sensitized Solar Cells. *Nano Today* **2011**, *6*, 91−109.

(16) Cheng, H.-M.; Chiu, W.-H.; Lee, C.-H.; Tsai, S.-Y.; Hsieh, W.-F. Formation of Branched ZnO Nanowires from Solvothermal Method and Dye-Sensitized Solar Cells Applications. *J. Phys. Chem. C* **2008**, *112*, 16359−16364.

(17) Baxter, J. B.; Aydil, E. S. Dye-Sensitized Solar Cells Based on Semiconductor Morphologies with ZnO Nanowires. *Sol. Energy Mater. Sol. Cells* **2006**, *90*, 607−622.

(18) Ko, S. H.; Lee, D.; Kang, H. W.; Nam, K. H.; Yeo, J. Y.; Hong, S. J.; Grigoropoulos, C. P.; Sung, H. J. Nanoforest of Hydrothermally Grown Hierarchical ZnO Nanowires for a High Efficiency Dye-Sensitized Solar Cell. *Nano Lett.* **2011**, *11*, 666−671.

(19) Guerin, V.-M.; Pauporte, T. From Nanowires to Hierarchical Structures of Template-free Electrodeposited ZnO for Efficient Dye-Sensitized Solar Cells. *Energy Environ. Sci.* **2011**, *4*, 2971−2979.

(20) Haller, S.; Suguira, T.; Lincot, D.; Yoshida, T. Design of a Hierarchical Structure of ZnO by Electrochemistry for ZnO-Based Dye-Sensitized Solar Cells. *Phys. Status Solidi A* **2010**, *207*, 2252−2257.

(21) Jiang, W.-T.; Wu, C.-T.; Sung, Y.-H.; Wu, J.-J. Room-Temperature Fast Construction of Outperformed ZnO Nanoarchitectures on Nanowire-Array Templates for Dye-Sensitized Solar Cells. *ACS Appl. Mater. Interfaces* **2013**, *5911*, 911−917.

(22) Chen-Hao, Ku; Jih-Jen, Wu Chemical Bath Deposition of ZnO Nanowire−Nanoparticle Composite Electrodes for Use in Dye-Sensitized Solar Cells. *Nanotechnology* **2007**, *18*, 505706.
(23) Dong, H.; Wang, L.; Gao, R.; Ma, B.; Qiu, Y. Constructing Nanorod-Nanoparticles Hierarchical Structure at Low Temperature as Photoanodes for Dye-sensitized Solar Cells: Combining Relatively Fast Electron Transport and High Dye-Loading Together. *J. Mater. Chem.* **2011**, *21*, 19389−19394.
(24) Chen, L.-Y.; Yin, Y.-T. Hierarchically Assembled ZnO Nanoparticles on High Diffusion Coefficient ZnO Nanowire Arrays for High Efficiency Dye-Sensitized Solar Cells. *Nanoscale* **2013**, *5*, 1777−1780.
(25) Anta, J. A.; Guillén, E.; Tena-Zaera, R. ZnO-Based Dye-Sensitized Solar Cells. *J. Phys. Chem. C* **2012**, *116*, 11413−11425.
(26) Xu, C.; Wu, J.; Desai, U. V.; Gao, D. Multilayer Assembly of Nanowire Arrays for Dye-Sensitized Solar Cells. *J. Am. Chem. Soc.* **2011**, *133*, 8122−8125.
(27) Bendall, J. S.; Etgar, L.; Tan, S. C.; Cai, N.; Wang, P.; Zakeeruddin, S. M.; Gratzel, M.; Welland, M. E. An Efficient DSSC Based on ZnO Nanowire Photo-Anodes and a New D-π-A Organic Dye. *Energy Environ. Sci.* **2011**, *4*, 2903−2908.
(28) Law, M.; Greene, L. E.; Radenovic, A.; Kuykendall, T.; Liphardt, J.; Yang, P. ZnO−Al_2O_3 and ZnO−TiO_2 Core−Shell Nanowire Dye-Sensitized Solar Cells. *J. Phys. Chem. B* **2006**, *110*, 22652−22663.
(29) Plank, N. O. V.; Snaith, H. J.; Ducati, C.; Bendall, J. S.; Schmidt-Mende, L.; Welland, M. E. A Simple Low Temperature Synthesis Route for ZnO−MgO Core−shell Nanowires. *Nanotechnology* **2008**, *19*, 465603.
(30) Plank, N.; Howard, I.; Rao, A.; Wilsin, M.; Ducati, C.; Mane, R. S.; Louca, R. R. M.; Bendall, J.; Greenham, N. C.; Miura, H.; Friend, R. H.; Snaith, H. J.; Welland, M. E. Efficient ZnO Nanowire Solid-State Dye-Sensitized Solar Cells Using Organic Dyes and Core−Shell Nanostructures. *J. Phys. Chem. C* **2009**, *113*, 18515−18522.
(31) Tang, H.; Matin, M. A.; Wang, H.; Deutsch, T.; Al-Jassim, M.; Turner, J.; Yan, Y. Synthesis and Characterization of Titanium-alloyed Hematite Thin Films for Photoelectrochemical Water Splitting. *J. Appl. Phys.* **2011**, *110*, 123511.
(32) Palomares, E.; Clifford, J. N.; Haque, S. A.; Lutz, T.; Durrant, J. R. Control of Charge Recombination Dynamics in Dye Sensitized Solar Cells by the Use of Conformally Deposited Metal Oxide Blocking Layers. *J. Am. Chem. Soc.* **2002**, *125*, 475−482.
(33) Diamant, Y.; Chappel, S.; Chen, S. G.; Melamed, O.; Zaban, A. Core-Shell Nanoporous Electrode for Dye Sensitized Solar Cells: The Effect of Shell Characteristics on the Electronic Properties of the Electrode. *Coord. Chem. Rev.* **2004**, *248*, 1271−1276.
(34) Fan, J.; Hao, Y.; Cabot, A.; Johansson, E. M. J.; Boschloo, G.; Hagfeldt, A. Cobalt(II/III) Redox Electrolyte in ZnO Nanowire-Based Dye-Sensitized Solar Cells. *ACS Appl. Mater. Interfaces* **2013**, *5*, 1902−1906.
(35) Ajuria, J.; Etxebarria, I.; Cambarau, W.; Munecas, U.; Tena-Zaera, R.; Jimeno, J. C.; Pacios, R. Inverted ITO-free Organic Solar Cells Based on p and n Semiconducting Oxides. New Designs for Integration in Tandem Cells, Top or Bottom Detecting Devices, and Photovoltaic Windows. *Energy Environ. Sci.* **2011**, *4*, 453−458.
(36) Guillén, E.; Peter, L. M.; Anta, J. A. Electron Transport and Recombination in ZnO-Based Dye-Sensitized Solar Cells. *J. Phys. Chem. C* **2011**, *115*, 22622−22632.
(37) Stiegler, J. M.; Tena-Zaera, R.; Idigoras, O.; Chuvilin, A.; Hillenbrand, R. Correlative Infrared−Electron Nanoscopy Reveals the Local Structure−Conductivity Relationship in Zinc Oxide Nanowires. *Nat. Commun.* **2012**, *3*, 1131.
(38) Sessolo, M.; Bolink, H. J.; Brine, H.; Prima-Garcia, H.; Tena-Zaera, R. Zinc Oxide Nanocrystals as Electron Injecting Building Blocks for Plastic Light Sources. *J. Mater. Chem.* **2012**, *22*, 4916−4920.
(39) Snaith, H. J. The Perils of Solar Cell Efficiency Measurements. *Nat. Photonics* **2012**, *6*, 337−340.
(40) Lin, C.-Y.; Lai, Y.-H.; Chen, H.-W.; Chen, J.-G.; Kung, C.-W.; Vittal, R.; Ho, K.-C. Highly Efficient Dye-sensitized Solar Cell with a ZnO Nanosheet-Based Photoanode. *Energy Environ. Sci.* **2011**, *4*, 3448−3455.
(41) Premaratne, K.; Kumara, G. R. A.; Rajapakse, R. M. G.; Karunarathne, M. L. Highly Efficient, Optically Semi-transparent, ZnO-Based Dye-Sensitized Solar Cells with Indoline D-358 as the Dye. *J. Photochem. Photobiol., A* **2012**, *229*, 29−32.
(42) Yella, A.; Lee, H.; Tsao, H.; Yi, C.; Chandiran, A. K.; Nazeeruddin, Md. K.; Diau, E. W.; Yeh, C. Y.; Zakeeruddin, S.; Grätzel, M. Porphyrin-Sensitized Solar Cells with Cobalt (II/III)−Based Redox Electrolyte Exceed 12% Efficiency. *Science* **2011**, *334*, 629−634.
(43) Puyoo, E.; Rey, G.; Appert, E.; Consonni, V.; Bellet, D. Efficient Dye-Sensitized Solar Cells Made from ZnO Nanostructure Composites. *J. Phys. Chem. C* **2012**, *116*, 18117−18123.
(44) Lin, L.-Y.; Yeh, M.-H.; Lee, C.-P.; Chou, C.-Y.; Vittal, R.; Ho, K.-C. Enhanced Performance of a Flexible Dye-sensitized Solar Cell with a Composite Semiconductor Film of ZnO Nanorods and ZnO Nanoparticles. *Electrochim. Acta* **2012**, *62*, 341−347.
(45) Rey, G.; Karst, N.; Doisneau, B.; Roussel, H.; Chaudouet, P.; Consonni, V.; Ternon, C.; Bellet, D. Morphological and Electrical Characterization of ZnO Nanocomposites in Dye-Sensitized Solar Cells. *J. Renewable Sustainable Energy* **2011**, *3*, 059101.
(46) Ku, C.-H.; Wu, J.-J. Electron Transport Properties in ZnO Nanowire Array/Nanoparticle Composite Dye-Sensitized Solar Cells. *Appl. Phys. Lett.* **2007**, *91*, 093117.
(47) Bisquert, J. Chemical Capacitance of Nanostructured Semiconductors: Its Origin and Significance for Nanocomposite Solar Cells. *Phys. Chem. Chem. Phys.* **2003**, *5*, 5360−5364.
(48) González-Pedro, V.; Xu, X.; Mora-Seró, I.; Bisquert, J. Modeling High-Efficiency Quantum Dot Sensitized Solar Cells. *ACS Nano* **2010**, *4*, 5783−5790.
(49) Jennings, J. R.; Liu, Y.; Wang, Q. Efficiency Limitations in Dye-Sensitized Solar Cells Caused by Inefficient Sensitizer Regeneration. *J. Phys. Chem. C* **2011**, *115*, 15109−15120.
(50) Neshataeva, E.; Kummell, T.; Bacher, G.; Ebbers, A. All-inorganic Light Emitting Device Based on ZnO Nanoparticles. *Appl. Phys. Lett.* **2009**, *94*, 091115.
(51) Bekeny, C.; Voss, T.; Gafsi, H.; Gutowski, J.; Postels, B.; Kreye, M.; Waag, A. Origin of the Near-Band-Edge Photoluminescence Emission in Aqueous Chemically Grown ZnO Nanorods. *J. Appl. Phys.* **2006**, *100*, 104317.
(52) Zimmler, M. A.; Voss, T.; Ronning, C.; Capasso, F. Exciton-Related Electroluminescence from ZnO Nanowire Light-Emitting Diodes. *Appl. Phys. Lett.* **2009**, *94*, 241120.
(53) Voss, T.; Bekeny, C.; Gutowski, J.; Tena-Zaera, R.; Elias, J.; Levy-Clement, C.; Mora-Sero, I.; Bisquert, J. Localized versus Delocalized States: Photoluminescence from Electrochemically Synthesized ZnO Nanowires. *J. Appl. Phys.* **2009**, *106*, 054304.
(54) Galoppini, E.; Rochford, J.; Chen, H.; Saraf, H.; Lu, Y.; Hagfeldt, A.; Boschloo, G. Fast Electron Transport in Metal Organic Vapor Deposition Grown Dye-sensitized ZnO Nanorod Solar Cells. *J. Phys. Chem. B* **2006**, *110*, 16159−16161.
(55) Martinson, A. B. F.; McGarrah, J. E.; Parpia, M. O. K.; Hupp, J. T. Dynamics of Charge Transport and Recombination in ZnO Nanorod Array Dye-sensitized Solar Cells. *Phys. Chem. Chem. Phys.* **2006**, *8*, 4655−4659.
(56) Feldt, S. M.; Gibson, E. A.; Gabrielsson, E.; Sun, L.; Boschloo, G.; Hagfeldt, A. Design of Organic Dyes and Cobalt Polypyridine Redox Mediators for High-Efficiency Dye-Sensitized Solar Cells. *J. Am. Chem. Soc.* **2010**, *132*, 16714−16724.
(57) Yum, J.-H.; Baranoff, E.; Kessler, F.; Moehl, T.; Ahmad, S.; Bessho, T.; Marchioro, A.; Ghadiri, E.; Moser, J.-E.; Yi, C.; et al. A Cobalt Complex Redox Shuttle for Dye-sensitized Solar Cells with High Open-Circuit Potentials. *Nat. Commun.* **2012**, *3*, 631.
(58) Burschka, J.; Dualeh, A.; Kessler, F.; Baranoff, E.; Cevey-Ha, N.-L.; Yi, C.; Nazeeruddin, M. K.; Grätzel, M. Tris(2-(1H-pyrazol-1-yl)pyridine)cobalt(III) as p-Type Dopant for Organic Semiconductors and Its Application in Highly Efficient Solid-State Dye-Sensitized Solar Cells. *J. Am. Chem. Soc.* **2011**, *133*, 18042−18045.

(59) Hardin, B. E.; Snaith, H. J.; McGehee, M. D. The Renaissance of Dye-sensitized Solar Cells. *Nat. Photonics* **2012**, *6*, 162−169.
(60) Ajuria, J.; Etxebarria, I.; Azaceta, E.; Tena-Zaera, R.; Fernandez-Montcada, N.; Palomares, E.; Pacios, R. Novel ZnO Nanostructured Electrodes for Higher Power Conversion Efficiencies in Polymeric Solar Cells. *Phys. Chem. Chem. Phys.* **2011**, *13*, 20871−20876.